Mat Res Innovat (2003) 7:245–252
DOI 10.1007/s10019-003-0260-4

ORIGINAL ARTICLE

Bingyun Li · Alexander Mukasyan · Arvind Varma

Combustion synthesis of CoCrMo orthopedic implant alloys: microstructure and properties

Received: 31 January 2003 / Revised: 30 May 2003 / Accepted: 3 June 2003 / Published online: 6 August 2003

Abstract Because of their excellent properties, such as corrosion resistance, fatigue strength and biocompatibility, cobalt-based alloys are widely used in total hip and knee replacements, dental devices and support structures for heart valves. In this work, CoCrMo alloys were synthesized using a *novel method* based on *combustion synthesis* (CS), an advanced technique to produce a wide variety of materials including alloys and near-net shape articles. This method possesses several advantages over conventional processes, such as *low energy requirements*, *short processing times* and *simple equipment*. The evaluated material properties included density and yield measurements, composition and microstructure analysis, hardness, friction and tensile tests. It was shown that *microstructure* of CS-material is *finer* and *more uniform* as compared to the conventional standard. It was also found that among various additives, Cr_3C_2 is the most effective one for increasing material hardness. In addition, synthesized CoCrMo alloys exhibited good friction and mechanical properties.

Keywords Bio alloys · Synthesis · Combustion · Microstructure · Mechanical properties

Introduction and relation to previous work

The $12 billion worldwide orthopedic industry is among the fastest-growing and most profitable segments of medical technology, whose sales are expected to increase in the 12% range over the next few years [1]. For example, in the United States alone, more than 400,000 hip and knee joints are replaced annually using artificial implants [2, 3]. According to different functional and biological requirements, a variety of materials are currently used in medicine. Metals and alloys, particularly cobalt-chromium and titanium alloys, as well as stainless steel are utilized for bone and joint implants. Among these, cobalt-based investment castings have been widely used in total hip and knee replacements, bone screws, staples, plates, dental devices, and support structures for heart valves. This is because cobalt-based alloys (Co-alloys) have the requisite good wear and corrosion resistance, fatigue strength and biocompatibility [4, 5, 6, 7].

These Co-alloys, complying with the ASTM F-75 standard, are produced by conventional casting technology [8], which is generally an energy- and time-intensive process, and the resulting materials are relatively expensive due to operating and capital equipment costs. Moreover, carbide precipitation represents the main strengthening mechanism in the as-cast conditions. However, in this process it is difficult to obtain uniform microstructure with finely distributed refractory carbides and thus segregation (e.g. networking and pooling) is often observed [9], which makes the materials difficult to hot work and may cause implant fracture.

Combustion synthesis (CS) is a novel technique to synthesize a wide variety of advanced materials that include alloys and near-net shape articles of ceramics, intermetallics, composites, and functionally graded products. This method is based on the concept that once initiated locally by means of a thermal source of short-time service, a highly exothermic wave of chemical interactions self-propagates through the heterogeneous reaction medium. The attractive features of CS are the high temperatures (usually 2,000–4,000 K), fast heating rates (e.g. 10^4 to 10^6 K/s), and short reaction times (on the order of seconds) [10, 11]. Therefore, as a practical alternative to conventional metallurgical processing and alloy development technologies, CS has several advantages, including (a) low energy requirements and simplicity of the process, (b) high product purity due to the expulsion of volatile impurities, chemical homogeneity

B. Li · A. Mukasyan · A. Varma (✉)
Department of Chemical and Biomolecular Engineering
and Center for Molecularly Engineered Materials,
University of Notre Dame,
Notre Dame, Indiana 46556, USA
e-mail: avarma@nd.edu
Tel.: +1-574-631-9825
Fax: +1-574-631-8366

and fine-scale microstructure, all owing to the unique CS conditions, and (c) its scale-up ability, which means commercial quantities can be produced efficiently. Moreover, CS possesses screening ability to synthesize new alloy compositions conveniently, rapidly and in any required amounts in order to evaluate desired material properties.

To date, a variety of products, including borides, carbides, composites and metallic alloys, have been produced commercially using CS technologies [11, 12]. The application of an external force, such as high inert gas pressure or centrifugal force (i.e., overload), during or after combustion is generally required to produce pore-free (porosity less than 1%) products [11, 13, 14, 15, 16, 17]. However, these techniques incur economic penalty owing to the complicated setup. Thus it is important to develop a simpler and more efficient method to synthesize pore-free materials by combustion reaction.

In this work, we describe in detail a novel efficient and flexible technique, *Low-Pressure Combustion Synthesis* (LPCS), to produce pore-free orthopaedic implant materials in a single step. Special attention is paid to phase separation mechanism during combustion of thermite systems, as well as to characterization of LPCS-alloys, including analysis of chemical composition, microstructure, hardness, friction and tensile properties.

Materials and methods

The synthesis conditions as well as methods used for materials characterization are described below. Note that the property measurements were conducted primarily in the laboratories of Zimmer, Inc. (Warsaw, IN).

Materials synthesis

Among various types of CS processes, thermite (or reduction) combustion synthesis was used in our study to produce Co-alloys. In general, this process involves oxides and reducing metals (Al, Mg, Zr, Ti, etc.) as reactants, as well as desired additives and described by the formula:

$$\sum_{i=1}^{n}(MO_x)_i^{(s)} + \sum_{i=1}^{r} Z_i^{(s)} \Rightarrow \sum_{j=1}^{k}(ZO_y)_j^{(s,l)} + \sum_{j=1}^{l} M_j^{(s,l)} + Q$$

where $(MO_x)_i^{(s)}$ is an oxide which reacts with a reducing metal $Z_i^{(s)}$, resulting in the appearance of desired reduced metal $M_j^{(s,l)}$ and another, more stable oxide $(ZO_y)_j^{(s,l)}$, along with heat liberated Q.

The following specific thermite (Co_3O_4-Cr-Mo) + Al system was selected for CS of Co-alloys:

$$3Co_3O_4 + 8Al + (xCo, yCr, zMo) \Rightarrow 4Al_2O_3 + (9 + x)\text{Co-alloys}$$

where Al is the reducing agent, and x, y and z coefficients can be varied to obtain the desired combustion temperature and product composition. For example, to control reaction temperature and rate, pure Co metal was added to the initial mixture as diluent. Based on thermodynamic analysis [18], the mole ratio of Co to (Co + Co_3O_4) equal to 0.5 was selected as an optimum reactant composition, which corresponds to combustion temperature up to 2,900 K with small amount gas phase products. Note that this temperature value is higher than the melting points of both products, i.e. Co-alloy ($T_{m.p.,Co} \sim 1{,}800$ K) and Al_2O_3 ($T_{m.p.,Al2O3} \sim 2{,}300$ K), which is important for full separation of alloy from oxide slag. Simultaneously, minimizing gas products leads to synthesis of desired pore-free materials. The Cr and Mo additives are required by the ASTM F75-98 standard specifications for cast Co-alloys. In addition, carbon black, graphite, as well as different carbides and nitrides were used to enhance material properties. The characteristics of the utilized reactant powders are listed in Table 1.

The precursors in desired ratio were thoroughly mixed to ensure homogeneity of the reaction medium, which was then uniaxially cold-pressed into 20 mm cylindrical pellets at pressure ~85 MPa to density in the range 2.9–3.3 g/cm^3. To eliminate the horizontal spreading of liquid products, as well as to avoid possible metal splash on reaction chamber wall, pellets were inserted in a 42 mm inner diameter quartz tube covered from both sides by ceramic (BN or SiO_2) plugs. The tube was then constrained in a specially designed fixture and placed in a stainless steel reaction chamber, 400 mm high and 320 mm inner diameter (see Fig. 1). Before reaction initiation, the chamber was sealed, evacuated and purged with inert gas for three cycles and finally filled with argon to the desired pressure. Tungsten coil, positioned ~2 mm above the pellet surface, was electrically heated until the reaction was initiated locally, followed by immediate power turn-off, while the reaction wave propagated along the sample.

In this work, typical LPCS-ingot was a disk ~40 mm diameter and ~10 mm height. For the same experimental conditions, at least 4 samples were synthesized to ensure reproducibility of obtained results. To investigate the influence of casting on LPCS-alloy properties, relatively large amount of materials (~5 kg) were synthesized using the developed LPCS technology as shown in Fig. 2, where individual ingots may also be seen. These ingots were further cast in specially designed ceramic mold (Fig. 3) using the conventional approach. Briefly, this process involved heating alloy up to 1,880 K in the electrical furnace, followed by casting into mold preheated to 1,250 K. After this, various shape and size specimens, arranged as a casting tree (Fig. 4), were obtained for further analysis and property evaluation. In some cases, LPCS samples were additionally treated under the following hot isostatic pressing (HIP) conditions: T = 1,463 ± 25 K under a pressure of

Table 1 Powder Characterization

Reactants	Particle size	Purity, %	Density, g/cm^3	M.P., K	B.P., K	Source
Co_3O_4	–400 mesh	99.7	6.11	1173	N/A	Alfa Aesar
Al	–325 mesh	99.5	2.70	933	2740	Alfa Aesar
Co	–325 mesh	99.8	8.92	1766	3373	Cerac Inc.
Cr	–325 mesh	99	7.19	2148	2755	Alfa Aesar
Mo	3–7 μm	99.95	10.22	2883	5833	Alfa Aesar
Cr_3C_2	–325 mesh	99.5	6.68	2163	4073	Cerac Inc.
TiN	–325 mesh	99.5	5.22	3203	N/A	Cerac Inc.
TiC	~2 μm	99.5	4.93	3413	N/A	Cerac Inc.
Graphite	<1 μm	99.9995	2.25	3970	N/A	Alfa Aesar
Carbon, Lampblack	N/A	N/A	N/A	N/A	N/A	Fisher Scientific

M.P.: Melting point, B.P.: Boiling point, N/A: Not available

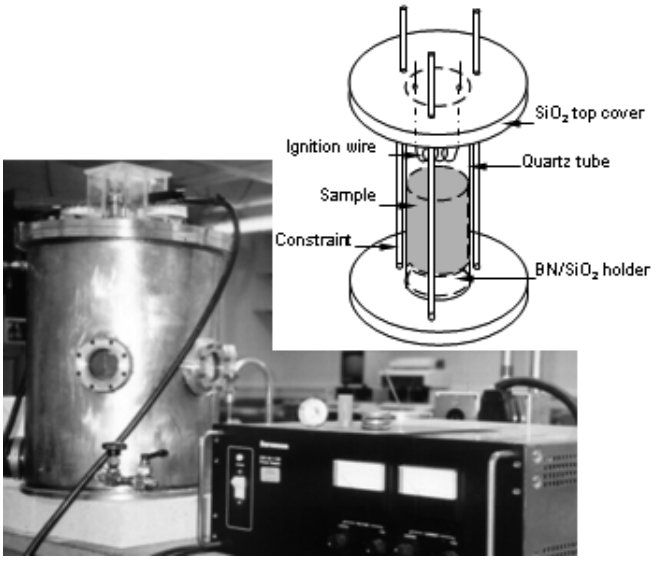

Fig. 1 The experimental setup. Inset shows details of the sample attachment fixture

Fig. 2 The LPCS-synthesized Co-alloy products (~5 kg)

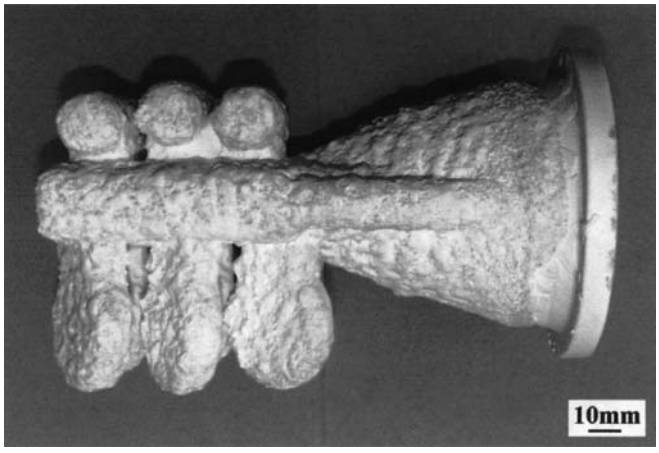

Fig. 3 The ceramic casting mold used in the present study

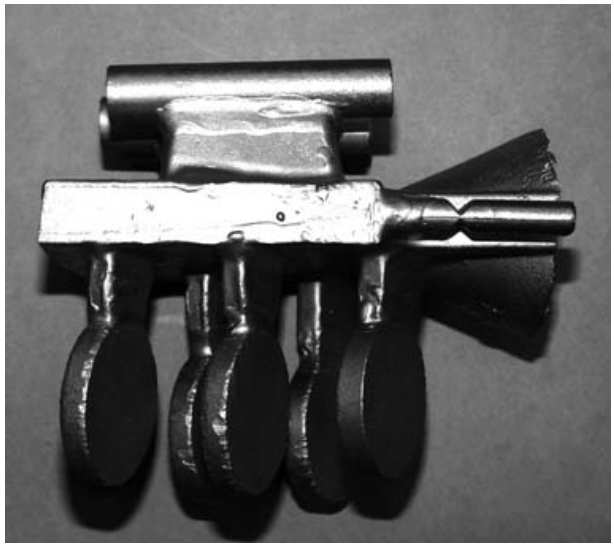

Fig. 4 The LPCS + Cast products

172 ± 2 MPa for 270 min, then cooled down to 922 K using inert gas under the load. Thus, in general, three types of samples were tested for various properties: as LPCS-Synthesized, LPCS + Cast and LPCS + HIP.

Materials characterization

The properties evaluated included density and yield measurements, composition and microstructural analysis, hardness, friction and tensile tests. Yield is defined as the ratio of the actual mass of produced metal alloy to the theoretical value corresponding to stoichiometric considerations, while density was determined using the Archimedes' principle. Optical and scanning electron microscopies were used to characterize sample microstructures. Rockwell hardness tests were performed based on the ASTM E18 standard at ambient temperature. The tensile tests were conducted in accordance with ASTM E8 standard specifications. For the latter, Co-alloys were machined into standard specimens with gauge length 25.4 mm and diameter 6.35 mm. Tensile tests were performed at ambient temperature in a computer-controlled electro-mechanical system using a 25.4 mm gauge length extensometer. Finally, friction tests against ultra high molecular weight polyethylene (UHMWPE) pins were conducted at ambient temperature using Pin-on-Disk machine with 100 g load, and ~5 cm/s speed. The initial surface roughness values of conventionally cast and LPCS samples used for friction test were 0.023 and 0.029 μm (Ra), and 0.368 and 0.427 μm (Rz), respectively.

Results

Combustion synthesis of Co-alloys

An important fundamental result of our research is that for each composition, a range of ambient inert gas pressure (typically lower than 1 atm) exists under which pore-free (>99% theoretical density) metal ingots can be synthesized by utilizing combustion technology with yield higher than 90% (see also Ref. 19). Briefly, Fig. 5a shows that with increasing ambient gas pressure initially alloy density decreases rapidly, while yield sharply increases, and both exhibit saturation. In the enlarged low-pressure region (Fig. 5b), one can see that at

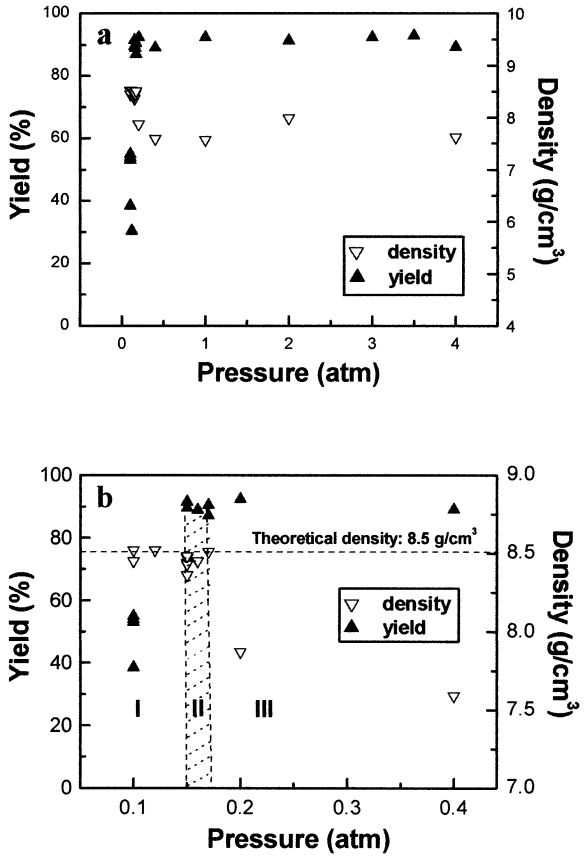

Fig. 5 (a) Influence of ambient gas pressure on basic Co-alloy density and yield. (b) Enlargement of low pressure region of (a). Region (I) has high density but low yield; region (III) has high yield but low density; region (II) exhibits high density and high yield simultaneously [19]

pressures lower than 0.15 atm (region I), a pore-free alloy is produced but the yield is lower than 60%. On the other hand, at pressures exceeding 0.18 atm (region III), the yield is more than 90% but the material density is too low owing to formation of large cavities in the ingot. Remarkably, a window of ambient gas pressures exists (region II) where *both* yield and density simultaneously possess acceptably high values. The related product configurations from each region are shown in Fig. 6. In regions I and II, slag formed in the shape of a thin-tube along the quartz container wall, while in region III Al_2O_3 cap formed on top of ingot. Thus from the viewpoint of process efficiency and product density, the optimum condition for the basic Co-alloy synthesis is ambient gas pressure in the range 0.15–0.18 atm.

Further, using the rapid screening ability of the developed LPCS technique, a wide range of material compositions was studied. For example, graphite, carbon black as well as several carbides (e.g., Cr_3C_2, TiC) were used as additives to enhance material properties. Table 2 lists the optimum initial gas pressures, as well as resulting yield and porosity values of several Co-alloys with various carbon additives. It appears that it is possible to find the optimum pressure range for synthesis of pore-free alloy with high yield in all cases. It may also be seen that increasing carbon black content increases the average optimum gas pressure. Further, for the same amount of added carbon, the lowest optimum pressure corresponds to the use of Cr_3C_2 additive.

The results of chemical analysis for different LPCS-alloys, along with F75 standard requirements, are shown in Table 3. It may be seen that the product composition can be easily controlled to match well with the ASTM

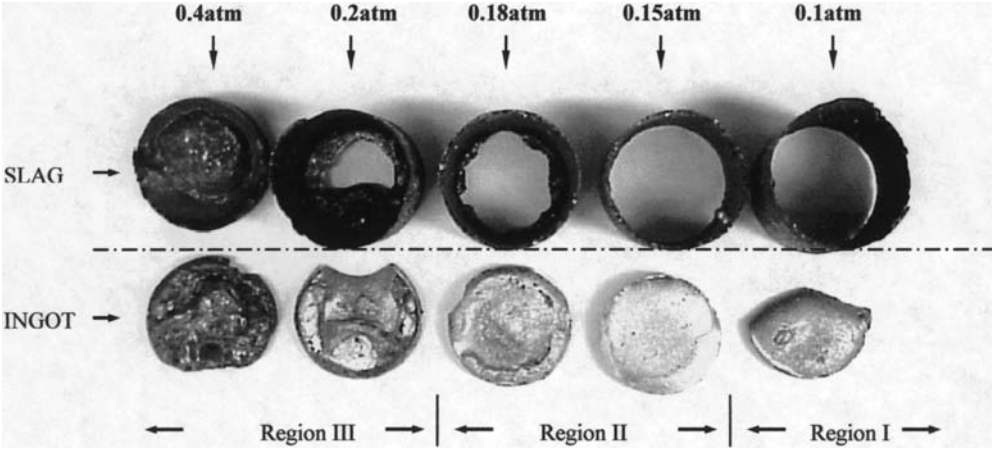

Fig. 6 Product configurations of basic Co-alloys synthesized by LPCS at different ambient gas pressures

Table 2 Synthesis Pressures for LPCS Co-alloys with Additives

Additive wt.% carbon	Carbon Black				Graphite 0.5	Cr_3C_2 0.5
	0	0.25	0.35	0.5		
Optimum pressure, atm	0.15–0.18	0.15–0.26	0.32–0.40	0.8–1.0	0.15–0.4	0.08–0.2
Yield, %	91	83	78	83	85	80
Porosity, %	<1	<1	<1	<1	<1	<1

Table 3 Chemical Compositions (wt.%) of Different Co-based Alloys

Elements	Co	C	Cr	Mo	Si	W	Al*	Fe	Mn	Ni	P	S	Ti	Cu	N
F75-98															
min	bal	…	27.0	5.0	…	…	…	…	…	…	…	…	…	…	…
max	bal	0.35	30.00	7.00	1.00	0.20	0.30	0.75	1.00	1.00	0.020	0.010	…	…	0.25
LPCS-1	bal	0.02	28.42	6.34	0.07	0.11	0.20	0.12	0.088	0.02	0.008	0.007	0.005	0.015	0.006
LPCS-C-1	bal	0.33	28.00	6.43	0.79	0.14	0.240	0.11	0.084	0.04	0.007	0.010	0.006	0.016	0.026
LPCS-C-2	bal	0.43	28.28	6.61	0.73	0.079	0.30	0.11	0.086	0.02	0.007	0.007	0.005	0.014	0.012
LPCS-C + Cast-1	bal	0.28	27.88	6.18	0.80	0.12	0.008	0.13	0.12	0.03	0.006	0.007	0.005	0.017	0.038
LPCS-C + Cast-2	bal	0.42	28.04	6.81	0.69	0.13	0.16	0.12	0.10	0.03	0.007	0.007	0.006	0.014	0.055

* present as Al_2O_3

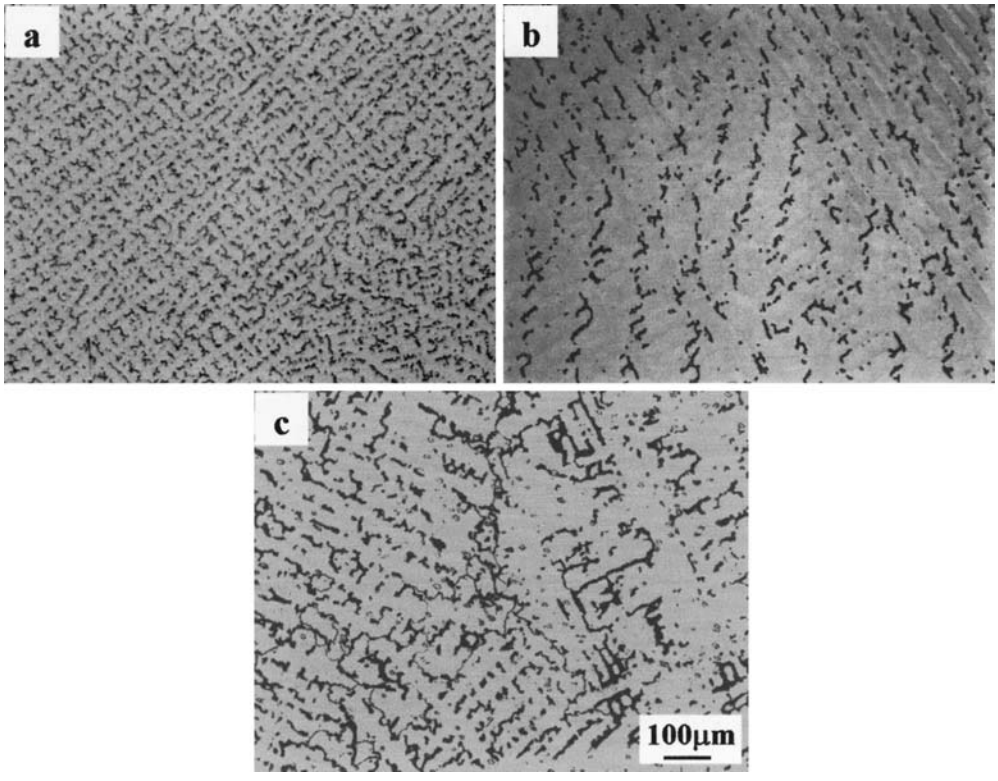

Fig. 7 Typical microstructures of pore-free Co-alloys with 0.33 wt.% C. (a) As LPCS-synthesized with Cr_3C_2 additive, (b) Conventional sample, (c) LPCS + Cast sample

specifications, and that the carbon content is adjustable up to high values. Further, all products have very low impurity levels, with only small residual Al present as Al_2O_3 inclusions, which decreases upon casting.

The typical microstructures of Co-alloys produced by LPCS and the conventional method are presented in Fig. 7. The microstructure of LPCS-alloy is finer and more uniform as compared to the conventional one (compare Fig. 7a and b), while casting leads to its coarsening (compare Fig. 7a and c).

Properties of LPCS-synthesized Co-alloys

As noted above, different additives were investigated to determine their influence on alloy properties. When carbon black or graphite is used, as shown in Fig. 8a, the hardness of Co-alloys increases with increasing carbon content, reaching ~31 HRc at 0.33 wt.% C. Among the various additives, at identical loading, Cr_3C_2 is the most effective one for increasing material hardness (Fig. 8b). Remarkably, with increasing carbon added as Cr_3C_2, the hardness of LPCS Co-alloys increases (Fig. 8c) to values that are significantly higher than with graphite or carbon black (Fig. 8a) and even the wrought Co-alloy [8]. For example, with 0.33 wt% carbon content, the LPCS-alloy with Cr_3C_2 additive has average hardness 46 HRc, approximately 50% higher than with C black or graphite addition.

Table 4 presents various mechanical properties for Co-alloys produced under different conditions. It appears that the hardness of LPCS-synthesized Co-alloy with Cr_3C_2 additive is higher than for all other samples, while elongation remains approximately the same. In general,

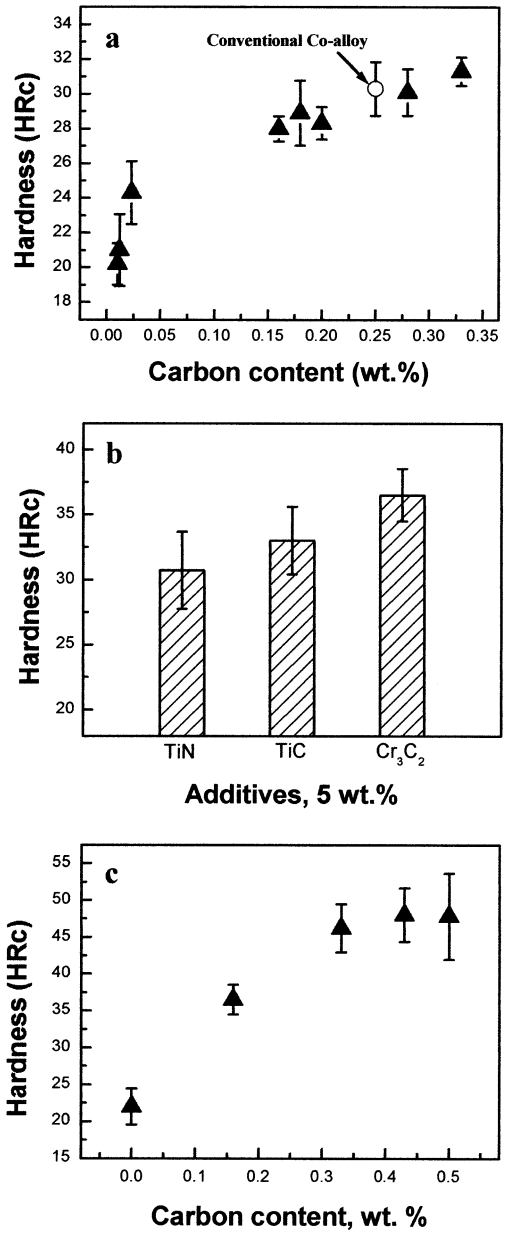

Fig. 8 Dependence of LPCS-synthesized alloys hardness on additives. (a) Hardness increases with increasing addition of graphite or carbon black. (b) For the same extent of carbide/nitride additives, Cr_3C_2 exhibits the most hardness enhancement. (c) Dependence of alloy hardness on Cr_3C_2 content (bars, standard deviation)

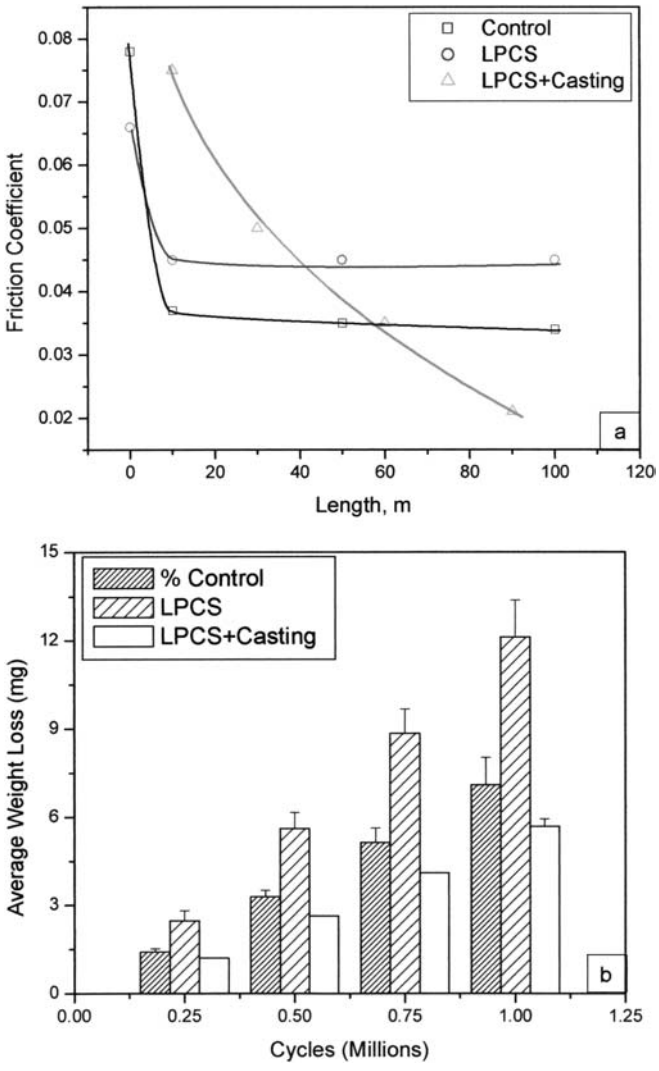

Fig. 9 Friction properties of LPCS-synthesized alloys against UHMWPE (bars, standard deviation)

although the other mechanical properties of LPCS-synthesized alloys are comparable to those of the conventional samples, the former possess relatively lower elastic modulus. After additional HIP or cast treatment, the LPCS-alloy shows decreased hardness and increased elastic modulus values. Further, LPCS + HIP samples

Table 4 Mechanical Properties of Co-based Alloys

Properties	LPCS-Synthesized		LPCS + HIP (0.02 wt.% C)	LPCS + Cast		Conventional (0.21 wt.% C + 0.17% N)
	(0.02 wt.% C)	(0.33 wt.% C*)		(0.28 wt.% C*)	(0.42 wt.% C*)	
Tensile strength, MPa	580	620	464	743	791	699
Yield strength (0.2%), MPa	363	512	323	471	540	485
Elongation, %	10	9	11	8	8	11
Reduction of area, %	9	12	15	10	7	17
Elastic Modulus, GPa	159	165	228	235	214	227
Hardness, HRc	23	46	23	32	34	32

*with Cr_3C_2 as additive

exhibit reduced strength and increased ductility, while LPCS + Cast alloys have higher tensile strength.

Finally, friction properties of LPCS-alloys with 0.33 wt.% C using Cr_3C_2 additive, as well as this alloy after casting (LPCS + Casting) and conventional (control) material are shown in Fig. 9a. As may be seen, the as-synthesized alloy, while having greater roughness and higher hardness, possesses comparable friction property with the conventional material, while after casting (LPCS + Casting) its friction coefficient is lower than that of control sample. The average data for the pin-on-flat wear test by using UHMWPE pin (see section Material characterization) are shown in Fig. 9b. The material produced from LPCS alloy followed by casting exhibits consistently lower average weight loss as compared to the conventional alloy.

Discussion

The distinctive feature of studied aluminum-thermite process is that combustion temperature is higher than the melting points of all reaction products, which contain two immiscible phases: relatively heavy metal alloy and light ceramic slag (Al_2O_3). Specifically, for the present system, the combustion temperature is ~2,900 K while melting points of products are $T_{m.p.,Co} \sim 1{,}800$ K and $T_{m.p.,\,Al2O3} \sim 2{,}300$ K. Note that both phases have essentially same volume in the melt, and complete phase separation between slag and alloy typically occurs in a few seconds.

In general, it is known that phase separation in thermite systems is affected by different parameters, including combustion temperature, heat losses and gravity (e.g. centrifugal acceleration) [13, 14]. However, for systems investigated in this work, it was shown that this process is controlled primarily by non-gravity driven mechanisms, such as surface tension and wetting ability [20], as well as by buoyancy, owing to difference in product densities ($\rho_{Co} = 8.5$ g/cm^3, $\rho_{Al2O3} = 2.8$ g/cm^3).

It is interesting that while Co-alloy always lies at the bottom of the container after phase separation, two types of slag (Al_2O_3) configuration were observed: as thin tube along the container wall or as cap on top of the metal ingot (Fig. 6). Let us discuss this issue in detail. As noted above, the pore-free alloy with high yield can be achieved only at relatively low ambient gas pressure, P_0 (see Fig. 5b). At high LPCS temperature (~2,900 K), impurities and part of the products are in gas phase (metal vapor, suboxides, carbon monoxide, etc.) and the intensive gasification causes an increase of gas pressure in the reaction medium. It is clear that pressure difference between inside and outside of the melted products increases with decreasing P_0. This pressure gradient (ΔP) is believed to control the formation of alloy microstructure, as well as the location of Al_2O_3 slag and the product mass loss (yield).

In one case, when P_0 is smaller than a certain critical value, P_{cr}^1, and thus ΔP is relatively large (e.g. more than weight of formed products), it leads to product splash (blow off) and as a result, while gas completely escapes from the melt (forming pore-free alloy microstructure), the yield is low (see region I, Fig. 5b). On the other hand, when P_0 exceeds another critical value, P_{cr}^2, no splash is detected during the process, however, solid Al_2O_3 cap forms first on top of the metal melt, leading to the formation of cavities and pores in the ingot and thus resulting in high yield but low density (see region III, Fig. 5b). In general, pores may form as a result of either shrinkage during solidification or entrapped gas by the crystallization of an Al_2O_3 cap at high temperatures. Our experiments show that the latter mechanism predominates.

It appears that only if initial gas pressure P_0 satisfies: $P_{cr}^1 \leq P_0 \leq P_{cr}^2$, one achieves pore-free (>99% theoretical density) alloy with high yield (>90%) (see region II, Fig. 5b). In this case, on one hand, moderate gas pressure difference leads to the formation of thin slag tube (Fig. 6) along the container wall, which permits continuous gas evolution from the melt, leading to pore-free product. On the other hand, the ΔP is not high enough to blow out metal alloy, providing high yield. For the basic Co-alloy composition, the lower and higher critical pressures are $P_{cr}^1 = 0.15$ atm and $P_{cr}^2 = 0.18$ atm, respectively.

Note that splash of products has frequently been observed during combustion of other thermite systems, and extremely high gas pressure and centrifugal force using specially designed setup have been applied to suppress this effect [21]. It is an important result of the present work that such irregularity can be successfully avoided simply by adjusting the initial ambient gas pressure. Note that for different reaction systems, the optimum gas pressure range can be identified based on the concept described above.

As seen from Table 2, the values of optimum ambient gas pressure are higher with additives. This occurs because, as thermodynamic calculations show, the amount of gas phase products increases with addition of carbon as well as carbides to the basic composition. Thus it was necessary to increase P_0 in order to keep the gas pressure difference in the optimum range, along with acceptably high yield. From this viewpoint, because carbon black possesses a substantially higher reactant surface area than graphite [22], it leads to more intense gasification and hence higher P_0 than with graphite.

As in conventional methods [23], the addition of carbon in any form increases the hardness of Co-alloys (see Fig. 8). However, the hardness values for alloys synthesized with Cr_3C_2 additive are significantly higher than those exhibited by other materials. For example, the hardness of LPCS-alloys with Cr_3C_2 additive is approximately 50% higher than that of conventional cast alloys with the same carbon content (0.33 wt.%). This can be explained based on the finer and more uniform distribution of carbides phases in metal matrix for LPCS-alloys with Cr_3C_2 additive (Fig. 7). It appears that Cr_3C_2, with melting point 2,168 K (compare with 3,800 K for C), which is much lower than the combustion temperature

~2,900 K (compare with ~1,900 K for conventional casting), melts and distributes uniformly in the alloy, with finer precipitation arising from the short LPCS period (few sec).

While hardness of LPCS-alloys with Cr_3C_2 additives, as discussed above, is higher, the other evaluated mechanical properties (see Table 4) compare favorably with the conventional alloys and meet ASTM F75 standards. After HIP, the strengths of LPCS-alloys decrease while the corresponding ductility and reduction in area increase. This may owe to the partial dissolution of grain boundary carbides, reduction of possible internal microvoids and growth of grain size during HIP process [24]. Moreover, cast treatment after LPCS, on one hand, leads to coarsening of carbide phases (Fig. 7) which decreases hardness, and on the other results in release of rapid cooling related internal stress which increases tensile strength.

Regarding wear/friction resistance, the friction coefficient against UHMWPE of wrought Co-alloy with hardness comparable to LPCS-alloy, is about 0.09 [25], almost twice that of the tested LPCS-samples (see Fig. 9). Moreover, in the alloy/UHMWPE bearing couple, increase in surface roughness leads to significantly increased wear [26, 27, 28]. In this context, note that the surface of tested LPCS-alloy was rougher (Ra = 0.029 μm, Rz = 0.427 μm) than that of conventional cast samples (Ra = 0.023 μm, Rz = 0.368 μm). Despite this, the friction properties of these materials are comparable. Further, the long-term friction coefficient of LPCS + casting alloy is at least 50% lower than the control sample (Fig. 9a), which results in lower weight loss (Fig. 9b). Thus, it is demonstrated that LPCS-based alloys have good friction properties.

Therefore, an analysis of various properties presented above allows one to conclude that for hardness, the as-synthesized LPCS-alloy is the best candidate. However, if ductility is the optimized parameter, then LPCS + HIP treatment should be considered. Finally, if tensile strength is important, then LPCS + Cast alloy is the choice.

Conclusions

The work presented here, along with our recent report [19], shows that a novel energy efficient Low Pressure Combustion Synthesis (LPCS) process to produce alloys useful for orthopedic implants has been developed. Optimum synthesis conditions for pore-free Co-alloys with high yields and high purity have been achieved. The LPCS-synthesized Co-alloy with Cr3C2 additive has fine microstructure, unusually high hardness, excellent friction property, and acceptable mechanical properties. This one-step LPCS-based process is simple, which suggests that its scale-up beyond the laboratory level would be straightforward. The materials synthesized by the combustion approach possess attractive properties, and are available for further biomedical evaluation.

Acknowledgements The financial support by the 21st Century Research & Technology Fund, State of Indiana, is gratefully acknowledged. We also thank Dr. Ravi Shetty, Zimmer, Inc., Warsaw, IN for his interest in this work and assistance with materials characterization.

References

1. Martinelli KA, Lemaitre DT, Lee TJ (2001, November 21) Orthopedic Industry: Update and Company Models. Merrill Lynch, New York, p 1
2. Saleh KJ (2001) Clinical Orthopedic and Related Research 392:153
3. Cushner F, Friedman RJ (1988) South Med J 81:1379
4. Keller JC, Lautenschlager EP (1986) Metals and alloys. In: von Recuum AF (ed) Handbook of biomaterials evaluation. Macmillan, New York, p 3
5. Granchi D, Ciapetti G, Stea S, Savarino L, Filippini F, Sudanese A, Zinghi G, Montanaro L (1999) Biomater 20:1079
6. Muster D, Hage-Ali M, Rie KT, Stucky T, Cornet A, Mainard D (2000) MRS Bull 25:25
7. Asphahani AI (1988) Corrosion of cobalt-base alloy. In: ASM metal handbook, 9th edition. ASM International, Metals Park, Ohio, 13:658
8. Shetty RH, Ottersberg WH (1995) Metals in orthopaedic surgery. In: Wise DL (ed) Encyclopedic handbook of biomaterials and bioengineering, Part B; Applications. Marcel Dekker, New York, p 509
9. Gómez M, Mancha H, Salinas A, Rodríguez JL, Escobedo J, Castro M, Méndez M (1997) J Biomed Mater Res 34:157
10. Munir ZA, Anselmi-Tamburini U (1989) Mater Sci Rep 3:277
11. Varma A, Mukasyan AS (1998) Combustion synthesis of advanced materials. In: Powder metal technologies and applications, ASM Handbook. ASM International, Materials Park, Ohio, p 523
12. Merzhanov AG (1990) Self-propagating high-temperature synthesis: twenty years of search and findings. In: Munir ZA, Holt JB (eds) Combustion and plasma synthesis of high-temperature materials. VCH, New York, p 1
13. Yukhvid VI (1992) Pure & Appl Chem 64:977
14. Odawara O (1996) Key Eng Mater 122:463
15. Seshadri R (2000) Metals Mater Proc 12:233
16. Ohmi T, Murota Y, Kudoh M (2001) Mater Trans 42:298
17. Yukhvid VI, Sanin VN, Nersesyan MD, Luss D (2002) Int J SHS 11:65
18. Shiryaev A (1995) Int J SHS 4:351
19. Varma A, Li B, Mukasyan A (2002) Adv Eng Mater 4:482
20. Lau C, Mukasyan AS, Varma A (2002) Proc Combust Inst 29:1101
21. Odawara O (1990) J Am Ceram Soc 73:629
22. Halverson DC, Ewald KH, Munir ZA (1995) J Mater Sci 30:3697
23. Tandon R (1999) Net-shaping of Co-Cr-Mo (F-75) via metal injection molding. In: Disegi JA, Kennedy RL, Pilliar R (eds) Cobalt-base alloys for biomedical applications.,ASTM STP 1365.: ASTM, West Conshohocken, PA, p 3
24. Mancha H, Gomez M, Castro M, Mendez M, Juarez J (1996) J Mater Syn Process 4:217
25. Huang P, Lopez HF (1999) Adv Sci Technol 28:111
26. Que L, Timmie LD, Parks NL (2000) J Biomed Mater Res 53:111
27. Saikko V, Calonius O, Keranen (2001) J Biomed Mater Res 57:506
28. Jinno T, Goldberg VM, Davy D, Stevenson S (1998) J Biomed Mater Res 42:20